Molecular Cell
Article

Mechanism of USP7/HAUSP Activation by Its C-Terminal Ubiquitin-like Domain and Allosteric Regulation by GMP-Synthetase

Alex C. Faesen,[1] Annette M.G. Dirac,[2] Anitha Shanmugham,[3] Huib Ovaa,[3] Anastassis Perrakis,[1] and Titia K. Sixma[1,*]
[1]Division of Biochemistry and Center for Biomedical Genetics
[2]Division of Molecular Carcinogenesis
[3]Division of Cell Biology
The Netherlands Cancer Institute, Plesmanlaan 121, 1066 CX Amsterdam, The Netherlands
*Correspondence: t.sixma@nki.nl
DOI 10.1016/j.molcel.2011.06.034

SUMMARY

The ubiquitin-specific protease USP7/HAUSP regulates p53 and MDM2 levels, and cellular localization of FOXO4 and PTEN, and hence is critically important for their role in cellular processes. Here we show how the 64 kDa C-terminal region of USP7 can positively regulate deubiquitinating activity. We present the crystal structure of this USP7/HAUSP ubiquitin-like domain (HUBL) comprised of five ubiquitin-like (Ubl) domains organized in 2-1-2 Ubl units. The last di-Ubl unit, HUBL-45, is sufficient to activate USP7, through binding to a "switching" loop in the catalytic domain, which promotes ubiquitin binding and increases activity 100-fold. This activation can be enhanced allosterically by the metabolic enzyme GMPS. It binds to the first three Ubl domains (HUBL-123) and hyperactivates USP7 by stabilization of the HUBL-45-dependent active state.

INTRODUCTION

The deubiquitinating enzyme (DUB) ubiquitin-specific protease 7 (USP7), also known as herpes virus-associated ubiquitin-specific protease (HAUSP), regulates the function of the tumor suppressor p53 that is mutated or inactivated in ~50% of human cancers (Vogelstein et al., 2000). USP7 removes ubiquitin from p53 itself, but also from the p53 E3 ubiquitin-ligase MDM2 (Cummins et al., 2004; Cummins and Vogelstein, 2004; Li et al., 2002, 2004). These combined effects determine functional p53 levels, creating an important role for USP7 in p53-dependent stress responses (Kon et al., 2010; Marchenko et al., 2007; Meulmeester et al., 2005). Precise regulation of USP7 expression and activity is therefore necessary for maintaining proper cell proliferation, and both up- and downregulation of USP7 inhibit colon cancer cell proliferation (Becker et al., 2008). USP7 also counteracts monoubiquitination of the transcription factor FOXO4 oncogene, and the phosphatase PTEN tumor suppressor, regulating their nuclear localization (Song et al., 2011; Trotman et al., 2007; van der Horst et al., 2006). Consequently, USP7 overexpression in prostate cancer was directly associated with tumor aggressiveness, most likely through PTEN mislocalization. Altogether, USP7 activity regulates important pathways for cell survival, proliferation, and apoptosis, misregulation of which often lead to tumorigenesis. Better understanding of USP7 activity may therefore contribute to insights in the role of these pathways in cancer.

USP7 is a cysteine isopeptidase of the ubiquitin-specific proteases (USP) family (Nijman et al., 2005). It contains an N-terminal TRAF/Math domain, a catalytic domain, and a 64 kDa C-terminal region (Figure 1A). The N-terminal TRAF domain directly interacts with the substrates of USP7 such as p53, MDM2, and TSPYL5 (Epping et al., 2011; Hu et al., 2006; Saridakis et al., 2005; Sheng et al., 2006). The catalytic domain of USP7 has the conserved fold of the USP family (Hu et al., 2002, 2006; Komander et al., 2008). It shows a papain-like architecture plus an extended, fingers-like domain that forms the ubiquitin binding pocket. Interestingly, the USP7 crystal structures show that the catalytic domain is maintained in a nonfunctional state, with the active site residues in a nonreactive conformation. The active conformation involves rearrangements of the catalytic domain that allow ubiquitin binding and organization of the catalytic triad, as shown in the structure of USP7 in complex with the suicide substrate ubiquitin aldehyde (Hu et al., 2002).

The C-terminal region of USP7 is essential for effective catalytic activity against a minimal synthetic substrate (Fernandez-Montalvan et al., 2007; Ma et al., 2010). It harbors additional MDM2 and p53 binding sites and promotes sequence-specific DNA binding of p53 (Ma et al., 2010; Sarkari et al., 2010). It was predicted to contain at least four domains with a ubiquitin-like (Ubl) β-grasp fold (Zhu et al., 2007), and a NMR structure of one of these is reported (2KVR). Ubl domains are also predicted at various positions in 16 additional USP enzymes. Two more Ubl domain structures are available: the N-terminal domains in USP14 (1WGG) and in USP4 (3JYU, residues 134–222). Among the USP family enzymes, USP7 is unique in containing a large number of consecutive Ubls.

Ubl domains share the ubiquitin fold but lack the C-terminal Gly-Gly residues required for conjugation to a target. Although many Ubl domains are found in the human genome, mostly as part of multidomain proteins, only few of these have been studied functionally (Grabbe and Dikic, 2009; Madsen et al., 2007). Among these, distinct subclasses have different functions (Burroughs et al., 2007). Most classes of Ubl domains, however,

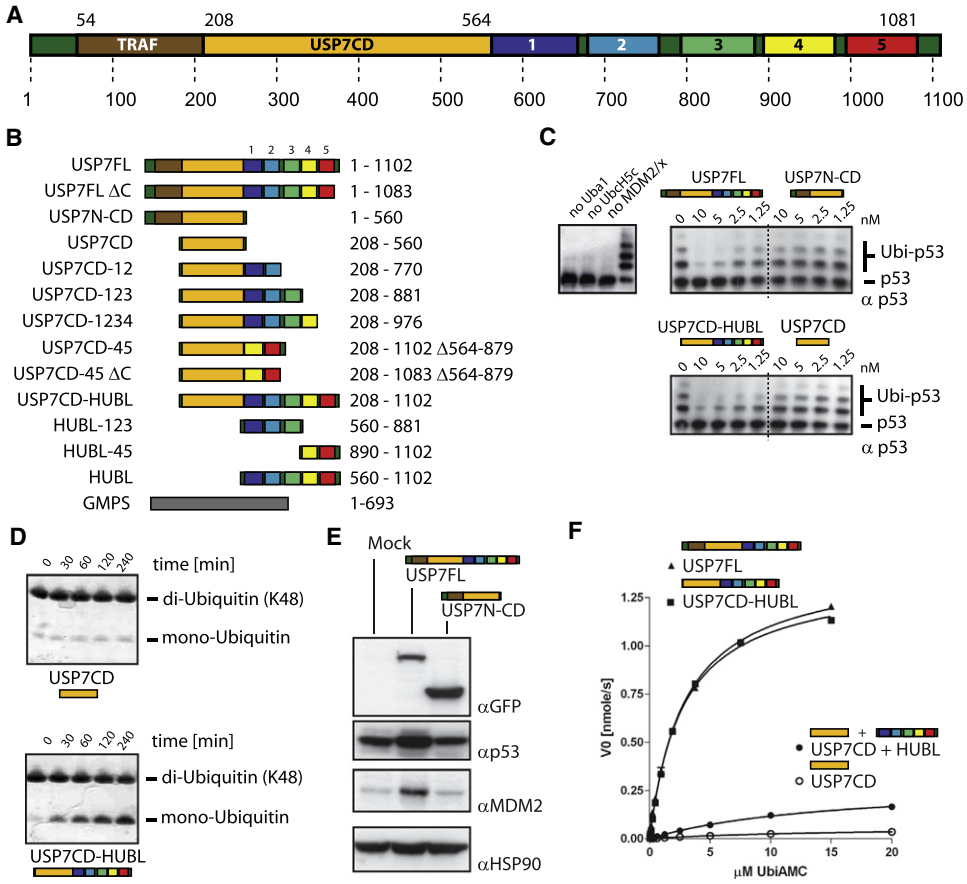

Figure 1. The HUBL Domain Is Essential for USP7 Activity

(A) USP7 contains a TRAF substrate binding domain (brown), a catalytic domain (orange), and five Ubl domains (rainbow).

(B) USP7 constructs used in this study.

(C) Only in the presence of the HUBL domain can p53 be deubiquitinated. The presence of the N-terminal TRAF domain has a minor additional effect.

(D) Using 10 μM diubiquitin and 1 nM USP7, only USP7CD-HUBL is able to hydrolyse the substrate to monoubiquitin.

(E) In U2OS cells, p53 and MDM2 protein levels increase compared to control levels by overexpression of full-length USP7. However, with overexpression of USP7N-CD, this stabilization is not observed. HSP90 was used as a loading control.

(F) Kinetic analysis of Ub-AMC hydrolysis shows similar activity for USP7FL and USP7CD-HUBL, while USP7CD is 90-fold decreased in K_M/k_{cat}. Kinetic parameters can be found in Table S1.

have not yet been characterized. Moreover, since different classes have only limited sequence similarity, they may have very different functions.

A number of interaction partners of USP7 have been identified (Sowa et al., 2009), but for most, neither function nor interaction site is known. So far, the TRAF domain seems dedicated to binding substrate proteins MDM2, p53, and TSPYL5. The C-terminal domain is also used for interactions, as was shown for Ataxin-1 (Hong et al., 2002) and the viral E3-ligase ICP0 (Canning et al., 2004). The metabolic enzyme GMP-synthetase (GMPS) interacts with USP7 in *Drosophila* (van der Knaap et al., 2005) and human cells (Sarkari et al., 2009). GMPS was found upregulated in tumorigenic cells (Boritzki et al., 1981; Weber et al., 1983) and together with USP7 is involved in cell survival, chromatin maintenance, and transcriptional regulation of ecdysteroid target genes (van der Knaap et al., 2010). This interaction promotes USP7 activity toward H2B as well as enhancing activity against p53 in *Drosophila*. The activation mechanism is unclear but possibly involves both general and target-specific aspects.

Here we investigate how Ubl domains in the C-terminal region of USP7 promote activity. We show that USP7 exists in two states, an active and an inactive state. In the active state the C-terminal Ubl domains HUBL-45 interact with a "switching loop" in the catalytic domain. We identified point mutations that interfere with the activation to validate its relevance in cells. Finally we show that GMPS can allosterically stabilize the interaction between HUBL-45 and the catalytic domain and thus promote the active state.

RESULTS

The HUBL Domain Is Essential for USP7 Activity In Vitro and In Vivo

To study the function of the 64 kDa C-terminal HUBL domain of USP7, we purified a series of different USP7 constructs

(Figures 1A and 1B) and compared their activity against ubiquitinated p53. In this assay, purified p53 was ubiquitinated in vitro with human MDM2/MDMX and then incubated with the USP7 constructs. p53 could only be efficiently deubiquitinated by USP7 constructs that contain the HUBL domain (Figure 1C, top panel). Removal of the N-terminal p53-binding domain (TRAF) does not affect the role of the HUBL domain and has a relatively limited influence on the activity in these experiments (Figure 1C, bottom panel).

We then analyzed the importance of the HUBL domain for activity against ubiquitin chains, by monitoring hydrolysis of K48-linked diubiquitin into monoubiquitin. Consistently, we saw robust activity in the presence of the HUBL domain, whereas in its absence no activity was observed (Figure 1D). Only when the concentration of the catalytic domain was 1000-fold increased could activity be observed (see Figure S1B available online). Thus the HUBL domain is essential for full enzymatic activity of the USP7 catalytic domain.

To study the in vivo significance of the HUBL domain, we transfected U2OS cells with GFP-fused full-length USP7 and USP7N-CD and investigated protein levels of two USP7 substrates, p53 and MDM2. Our experiments showed an accumulation of p53 and MDM2 in the presence of full-length USP7 compared to USP7N-CD (Figure 1E). This suggests that the HUBL domain is required to deubiquitinate p53 and MDM2, and thereby prevents degradation, resulting in a net stabilization. This shows that the HUBL domain is important for the activity of USP7 in vivo and therefore essential for its biological function.

To quantify the HUBL-mediated activation, we used a minimal synthetic substrate, ubiquitin fused to a C-terminal fluorescent group, 7-amido-4-methylcoumarin (Ub-AMC). Full-length USP7 and a construct that lacks the TRAF domain (USP7CD-HUBL) showed very similar activity, with similar Michaelis-Menten kinetic parameters (V_{max} 1.4 nmole s^{-1} and K_M 3 μM) (Figure 1F and Table S1). In contrast, the catalytic domain alone (USP7CD) was much less active, with a decrease in V_{max} to 0.06 nmole/s (22-fold) and an increase in K_M to 15 μM (5.5-fold). Altogether, the enzyme efficiency (k_{cat}/K_M) decreases 120-fold, suggesting that the C-terminal HUBL domain is essential to achieve full enzymatic efficiency and therefore activates the catalytic domain.

Since all USP7 constructs eluted as monomers from gel filtration, it is likely that this activation occurs within the same molecule. However, we wondered whether the HUBL domain could activate the catalytic domain when it is not part of the same chain, in *trans*. First we showed that the HUBL domain itself has no DUB activity on Ub-AMC, and then we mixed the catalytic domain with the HUBL domain. Adding 10 μM HUBL domain to the catalytic domain resulted in a 2-fold increase of catalytic turnover (Figure S1A). However, when adding a higher excess of the HUBL domain (50 μM), a clear activation can be observed (Figure 1F). This result shows that the catalytically inactive HUBL domain can indirectly activate the USP7 catalytic domain also in *trans*, at least at high concentrations.

To exclude the possibility that the observed in vitro activation was due to assay conditions, we tested the effect of pH and salt concentration. The USP7 activity is strongly dependent on pH (Figure S1C), with an optimum between pH 8 and 9, and also shows considerable dependence on ionic strength (Figure S1D). Since p53 is responsible for stress responses, these pH and ionic strength dependencies may well be relevant in cells. However, the presence of the HUBL domain has no effect on the pH response and only a mildly positive effect on the response to salt (Figures S1C and S1D, right panels). Thus, although activation may have an electrostatic component, we concluded that neither ionic strength nor pH effects explain how the activation is achieved.

Altogether these data confirm and extend the observation that the C-terminal domain is essential for full activity against Ub-AMC. As expected, the N-terminal TRAF domain increases the activity against p53, but not against the minimal target Ub-AMC, and has therefore no effect on the HUBL activation itself. We thus show that the catalytically inactive HUBL domain indirectly activates USP7 catalytic domain in a target-independent manner.

The USP7 HUBL Structure Shows Five Ubl Domains in Three Units

To investigate the mechanism underlying USP7 activation by its HUBL domain, we determined the crystal structure of the HUBL domain (residues 560–1102) using single anomalous dispersion (SAD) phasing from selenomethionines (Figures 2A and 2B). The final model was refined to 2.7 Å with R_{free} of 0.216 (Table 1), and includes residues 560–1083 with no Ramachandran outliers. The HUBL domain comprises five modules with the ubiquitin-like ββαβαβ-fold, one more than previously predicted based on consensus fold recognition (Zhu et al., 2007). The Ubl domains adopt an extended conformation, linked through regions of varying size that contain either one or two α helices. The helices connecting HUBL-2 and -3 interact with HUBL-2 (Figure S2A), but otherwise these linkers have little contact with the individual domains.

The Ubl domains closely resemble ubiquitin (rmsd 1.9–2.5 Å, Figure 2C and Figures S2B and S2C) and SUMO-2 (rmsd 2.2–2.9 Å), according to SSM (Krissinel and Henrick, 2004) and DALI (Holm et al., 2008) structural similarity searches against all structures in the PDB. Despite the structural similarities, the sequence identities with ubiquitin are very limited, varying from 6% to 19% (Figure S2B). There are no obvious specific resemblances to other ubiquitin-like domains beyond the conserved fold, and hence it is not obvious that there is a shared function with other classes of Ubl domains.

Although the five Ubl domains share the ubiquitin fold, they are no more similar to each other than to other ubiquitin-like structures (rmsd 2.1–2.9 Å), and they are widely divergent in sequence (3%–15% sequence identity) (Figure S2B). This leads to large variations in charge distribution, such that under physiological conditions HUBL-1 and -2 are negatively charged (calculated pI 4.4 and 4.5, respectively), HUBL-3 is positively charged (pI 9.8), and HUBL-4 and -5 are neutral (pI 5.6 and 6.0, respectively) (Figure S5D). Mutations in these charged patches do not affect the enzymatic activity of USP7 (Figure S5C), although they may play a role in other functions of the protein, such as protein-protein interactions with its binding partners.

The HUBL domain is organized in an elongated arrangement, in which HUBL-3 has limited contacts with the other domains (Figure 2B), and HUBL-1 and -2, as well as HUBL-4 and -5,

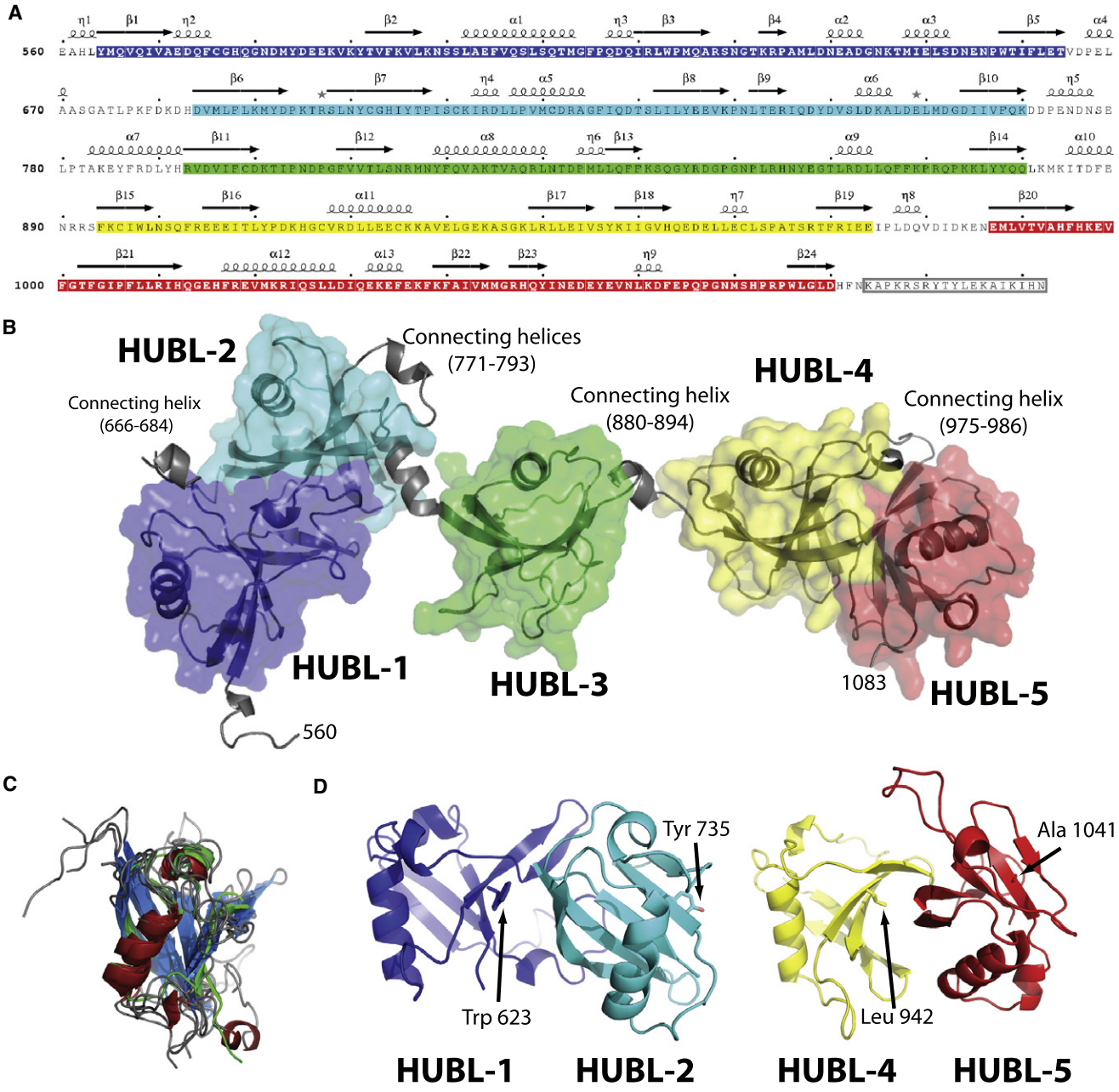

Figure 2. Crystal Structure of the HUBL Domain Shows Five Ubl Domains

(A) Secondary structure assignment of the HUBL domain. The residues are colored to the corresponding Ubl. Disordered residues (1084–1102) are boxed.

(B) Cartoon representation of the HUBL domain with surface representation of the Ubls. See Table 1 for crystallographic information.

(C) Structure superposition shows that the Ubls share the β-grasp fold with ubiquitin, with variations in the length of the loop regions (red, α helix; blue, β strand; green, ubiquitin).

(D) Di-Ubl units HUBL-12 and HUBL-45 are somewhat similar in Ubl orientation, showing a relative 30 degree rotation of HUBL-5 compared to HUBL-2. The ubiquitin Ile44 equivalents in the HUBL domains are labeled and depicted in sticks.

form di-Ubl units. Analysis with PISA (Krissinel and Henrick, 2004) shows that the di-Ubl interfaces bury a large surface area (total ~1200 and ~740 Å^2, respectively) with negative solvation energies ΔiG (Figure S2D), suggesting that they are stable in solution. This was supported by the degradation pattern of semi-purified USP7CD-HUBL, which degrades to three stable fragments that correspond to the masses of USP7CD-123, USP7CD-12, and USP7CD (Figure S2E). From this we concluded that the HUBL domain is organized in a 2-1-2 fashion that contains three units: HUBL-12, HUBL-3, and HUBL-45.

Structural comparison of these di-Ubl units reveals that HUBL-12 and HUBL-45 are similarly arranged (Figure 2D). Superposing

Table 1. Crystallography Details

Data Collection Statistics	HUBL (Native)	HUBL (SeMet)
Wavelength (Å)	0.873	0.979
Resolution (Å)	2.7	3.0
Space group	$P2_12_12_1$	$P2_12_12_1$
Cell dimensions: a, b, c (Å)	79.98, 82.31, 150.63	79.54, 81.38, 150.10
Resolution limits (Å)	39.7–2.7 (2.85–2.7)	45.33–2.99 (3.16–3.0)
R_{merge} (%)	7.2 (69.3)	6.2 (32.7)
I/σI	11.8 (2.0)	26.2 (7.0)
Completeness (%)	100 (99.9)	99.5 (97.0)
Redundancy	4.5 (4.6)	13.1 (12.8)
Refinement		
Unique reflections (#)	27,939	20,203
Protein atoms (#)	4,340	
Waters (#)	129	
R_{work}/R_{free} (%)	19.1/21.6	
Rmsd from Ideal Geometry		
Bond lengths[a]	0.009	
Bond angles[a]	1.07	
Ramachandran statistics (preferred/allowed/outliers)[a]	514/15/0	

Highest-resolution shell is shown in parentheses.
[a] Calculated using MolProbity.

the N-terminal domains HUBL-1 and HUBL-4 shows that equivalent interfaces are buried on the first Ubl in each pair, including the residue that is equivalent to the canonical Ile-44 of ubiquitin (Trp-623 and Leu-942, respectively). The second Ubl domains do not bury their Ile-44 equivalent residues (Tyr 735 and Ala 1041), and they are arranged slightly differently with a relative rotation of ~30 degrees resulting in small differences in detailed contacts. In both di-Ubl units the interfaces are mediated by extensive hydrophobic contacts as well as hydrogen bonds and electrostatic interactions (Figure S2D). This suggests that these di-Ubl units are functionally relevant.

SAXS Analysis Suggests Flexibility and Interaction between USP7CD and HUBL

We were intrigued by the extended structure of the HUBL domain and wondered whether it was relevant in solution. To address this question, we used small-angle X-ray scattering (SAXS).

When we compared SAXS curves recorded for the USP7CD, HUBL-123, and HUBL-45 domains to scattering curves calculated from their corresponding crystal structures, we obtained a good fit between the experimental and calculated curves (Figure 3A). The calculated molecular weights (Mw), radii of gyration (Rg), and maximum interatomic distance (Dmax) also correspond well with the expected values (Figure 3B), with only the Rg of HUBL-45 ~30% larger than expected from the structure. These data show that USP7CD, HUBL-123, and HUBL-45 are structurally stable subdomains of USP7 also in solution.

In contrast, the scattering curve for the complete HUBL domain does not fit the calculated scattering curve (Figure 3A). The interatomic distance probability distribution *P(r)* shows a nonsymmetrical shape, including a significant proportion of long distances (Figure 3C). This suggests that the extended conformation is retained in solution. Since rigid body modeling did not yield a single model, we conclude that the structure of the HUBL domain in solution is not static, most likely exhibiting considerable flexibility between the two stable domains, HUBL-123 and HUBL-45.

The HUBL domain and USP7CD-HUBL have a similar radius, with the HUBL domain being marginally smaller as expected (Figures 3B and 3C). However, in the USP7CD-HUBL domain *P(r)* plot (Figure 3C) the asymmetry due to long interatomic distances mostly disappears, indicating a more compact molecule, despite the addition of the catalytic domain. This suggests that the HUBL domain folds back to the catalytic domain, resulting in a more compact shape. Since rigid body modeling did not yield a single solution, the interaction between the catalytic domain and the HUBL domain could be dynamic.

HUBL-45 Is Sufficient for USP7 Activation

To identify the minimal region in the HUBL domain that is required for activation of the USP7 enzymatic activity, we produced C-terminal deletion constructs (Figure 1B). Upon deletion of the last one or two Ubl domains, the resulting USP7CD-1234 and USP7CD-123 has a severely compromised catalytic turnover, similar to the catalytic domain alone (Figure 4A). As HUBL-45 is an independent folding unit that seemed essential for in vitro activity, we tested if deleting it would affect USP7 function in vivo.

After transfecting U2OS cells with full-length USP7, USP7N-CD, or USP7N-CD-123, we monitored p53 and MDM2 protein levels. Our experiments showed an accumulation of p53 and MDM2 in the presence of the full-length USP7, which is not observed in absence of HUBL-45 (USP7N-CD-123) (Figure 4B), suggesting that it is required to deubiquitinate p53 and MDM2. This shows that HUBL-45 is essential for USP7 function in vivo.

Then we analyzed whether HUBL-45 alone is enough to reconstitute full activity. We deleted HUBL-123, coupling the HUBL-45 unit directly to the catalytic domain via a 2 amino acid linker (USP7CD-45). This variant had V_{max} and K_M values almost identical to the complete USP7CD-HUBL (Figure 4D) in the Ub-AMC assay. In addition, USP7CD-HUBL and USP7CD-45 have similar efficiency against a diubiquitin substrate (Figure 4C). These results show that HUBL-45 is sufficient to reconstitute the USP7 activation.

HUBL-45 consists of the di-Ubl unit and a flexible C-terminal 19 residue peptide that is disordered in the crystal structure. When we deleted this C-terminal tail of HUBL-45 (USP7CD-45ΔC) we observed a greatly reduced activity, similar to USP7CD (Figure 4A), showing that the C-terminal peptide is critical for the activation. To see whether this peptide alone was sufficient to promote activation, we performed in *trans* activation experiments with Ub-AMC using the peptide alone versus complete HUBL-45, including the peptide. In these assays (Figure S3A), the peptide marginally activates USP7CD in *trans*, whereas the full HUBL-45 domain provides robust levels of activation (Figure S3A). Therefore, we conclude that the C-terminal activation peptide is essential to increase the activity of USP7CD, but only in the context of HUBL-45.

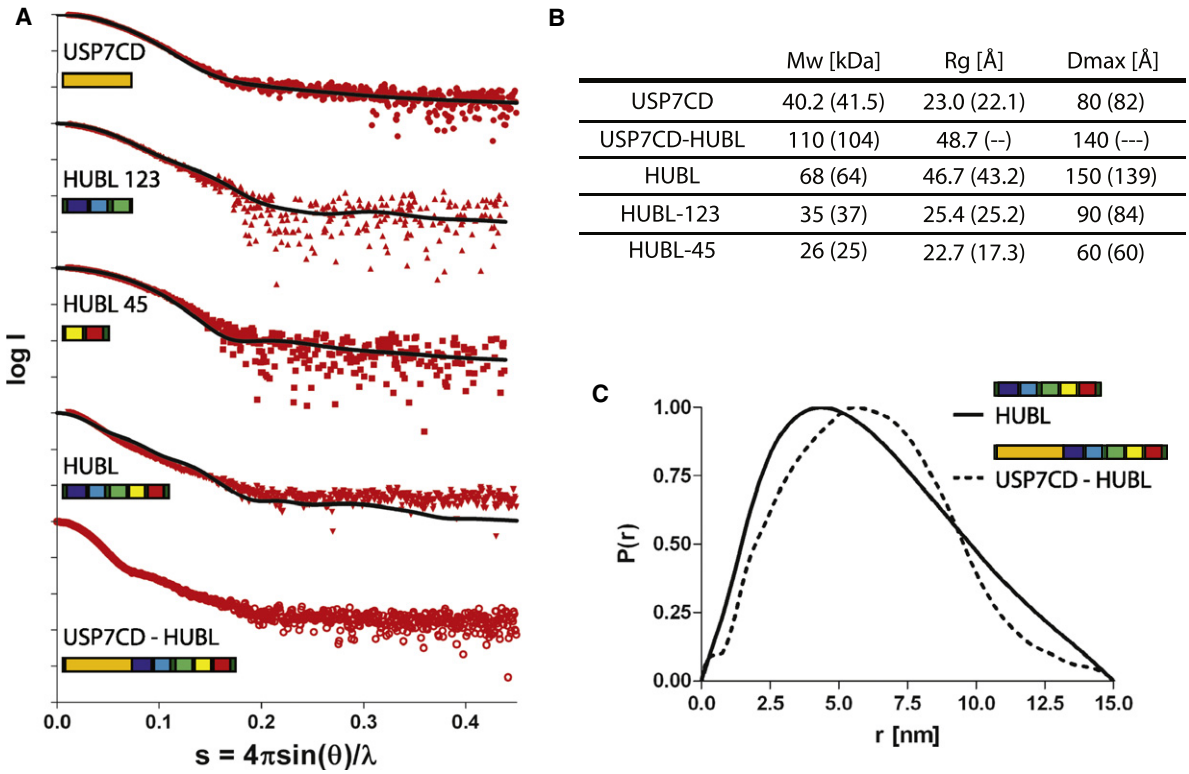

	Mw [kDa]	Rg [Å]	Dmax [Å]
USP7CD	40.2 (41.5)	23.0 (22.1)	80 (82)
USP7CD-HUBL	110 (104)	48.7 (--)	140 (---)
HUBL	68 (64)	46.7 (43.2)	150 (139)
HUBL-123	35 (37)	25.4 (25.2)	90 (84)
HUBL-45	26 (25)	22.7 (17.3)	60 (60)

Figure 3. SAXS Analysis of the HUBL Domain

(A) Scattering curves of the USP7 fragments (red symbols) with corresponding scattering curves calculated from the crystal structures (black lines).

(B) Overview of the SAXS analysis results.

(C) The symmetrical interatomic distance probability distribution (P(r)) of USP7CD-HUBL shows that it has less extended shape than the HUBL domain, indicating that the HUBL domain folds back onto the CD.

Collectively, the activation of the catalytic domain and the SAXS data imply that the activation mechanism is through a direct interaction between the catalytic domain and HUBL-45. Indeed, when using a surface plasmon resonance (SPR) binding assay with immobilized GST-USP7CD, we observed a 50 μM dissociation constant (K_d) for HUBL-45 (Figure 4E), in agreement with the concentrations required for *trans* activation by the HUBL domain (Figure 1F and Figure S3A). When the flexible C-terminal peptide was removed (HUBL-45ΔC), the affinity for the catalytic domain did not change (Figure 4E). Since no binding was detected between the catalytic domain and the peptide (Figure S3B), we concluded that although the peptide is essential for activity, the HUBL-45 di-Ubl unit is required for binding to the catalytic domain. This brings the flexible C-terminal activation peptide close to the catalytic domain, resulting in its activation.

The HUBL Domain Promotes Ubiquitin Binding

When considering the mechanism of USP7 activation, we realized that the lower K_M value in the catalytically efficient constructs suggested an increase in substrate affinity. Therefore we tested whether the HUBL domain affected the ubiquitin affinity of USP7CD. We incubated with the suicide substrate ubiquitin-VME (20 μM) (Borodovsky et al., 2001). While USP7CD alone was loaded only partially, USP7CD-45 loading was essentially complete (Figure S4A).

Since this could indicate an increase of ubiquitin affinity, we decided to validate this by SPR experiments. Neither USP7CD nor USP7CD-12 shows appreciable ubiquitin binding, with almost no responses measured up to 17 μM, suggesting very little affinity for ubiquitin (Figure 5A and Figure S4B). Also, no ubiquitin binding was observed for the HUBL domain itself (Figure 5A). However, the catalytically efficient USP7CD-HUBL construct showed a clear association and dissociation from ubiquitin. Both the kinetic and equilibrium data could be fitted with a K_d of 1.5 μM (Figures 5B and 5E). This indicates that the catalytic and HUBL domains cooperate to achieve ubiquitin binding. USP7CD-45 also binds ubiquitin with a K_d of 4 μM, similar to USP7CD-HUBL (Figures 5C and 5E), confirming that HUBL-45 is sufficient for the activation of USP7. Interestingly, although these Ubl domains may resemble ubiquitin, they do not compete for ubiquitin binding to USP7. Instead, they promote this interaction.

In the kinetic analyses, we observed that the catalytic domain and the HUBL domain cooperate in *trans* (Figure 1F). To test if that also translates to ubiquitin binding, different concentrations of USP7CD were flowed over the GST-ubiquitin chip in the presence of 50 μM HUBL. A partial reconstitution of the ubiquitin

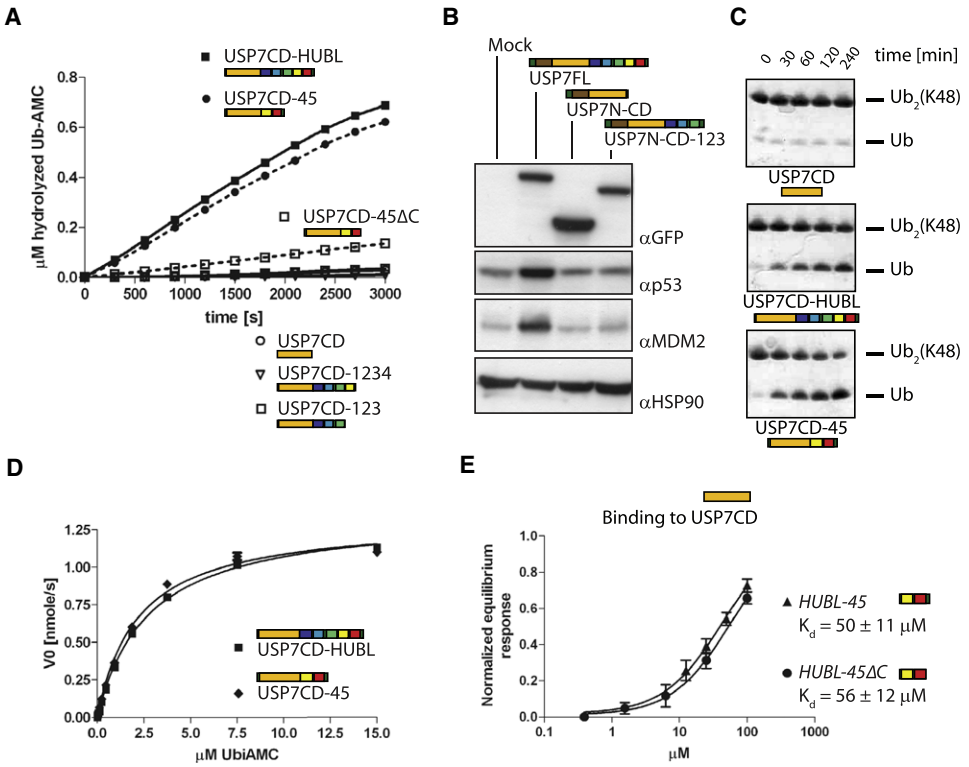

Figure 4. HUBL-45 Is Sufficient for Activation

(A) Any C-terminal deletion reduces activity to similar levels as USP7CD in Ub-AMC assays. However, the USP7CD-45 construct showed activity similar to that of USP7CD-HUBL. Removing the C-terminal peptide (USP7CD-45ΔC) resulted in greatly reduced activity.

(B) Loss of HUBL-45 reduces USP7 activity in U2OS cells: protein levels of p53 and MDM2 did not increase as seen with the wild-type full-length USP7. HSP90 was used as a loading control.

(C) USP7CD-HUBL and USP7CD-45 have similar activity toward 10 μM diubiquitin (K48), while USP7CD did not show any activity.

(D) USP7CD-45 still showed full activity in Ub-AMC assays.

(E) SPR binding experiments show an interaction with a K_d of 50 (±11) μM between GST-USP7CD and HUBL-45.

binding to a K_d of 13 μM was achieved, confirming that *trans* activation of the catalytic domain translates in an increased ubiquitin affinity (Figures 5D and 5E). The observed ubiquitin affinities correlate with the K_M values for Ub-AMC derived in the kinetic analysis, and therefore show that the increase of K_M can be explained by the increase of K_d (Table S1).

Point Mutants Prevent HUBL Autoactivation

To understand how HUBL-45 conveys the activation to the catalytic domain, we used site-directed mutagenesis and tested a number of different options (Figure S5). In USP7 the residues forming the catalytic triad adopt an inactive conformation (Hu et al., 2002) (Figure S5A). However, upon ubiquitin binding, the active site is remodeled to the active conformation. With this conformational change a small loop close to the active site (residues 285–291), that we name "switching loop," shows dramatic changes (Figure 6A).

We mutated several residues in this switching loop, in the context of both USP7CD and USP7CD-45, and tested their activity using Ub-AMC (Figure 6B and Table S1). These mutations show a limited activating effect when tested in the catalytic domain alone. However, in the context of USP7CD-45, two switching loop mutants, W285D and E286A, greatly reduce the activation effect conferred by HUBL-45. Moreover, the W285D E286A double mutant has a greatly reduced ubiquitin affinity (Figure 6D and Figures S4C and S4D).

The 19 residues in the flexible C-terminal peptide of HUBL-45 are essential for the activation (Figure S3A and Figure 6C). Several single-point mutants of conserved residues displayed a reduction in activating capacity (Figure 6C). Strikingly, the single-point mutant I1100S completely abolished the HUBL activation and greatly reduced ubiquitin binding (Figure 6C, Figure S4D, and Table S1). Consistently, overexpressing these USP7 mutants in U2OS cells completely abolished the stabilization of p53 and MDM2 observed for the wild-type enzyme (Figure 6E). This shows that, although they are not in direct contact with ubiquitin, both the switching loop and the C-terminal peptide of the HUBL domain are required for the HUBL-mediated increase of activity and ubiquitin affinity.

GMPS Binds to HUBL-123 and Allosterically Promotes Activation

Due to the intrinsic flexibility and weak interactions with the catalytic domain, the HUBL domain may not always be in the

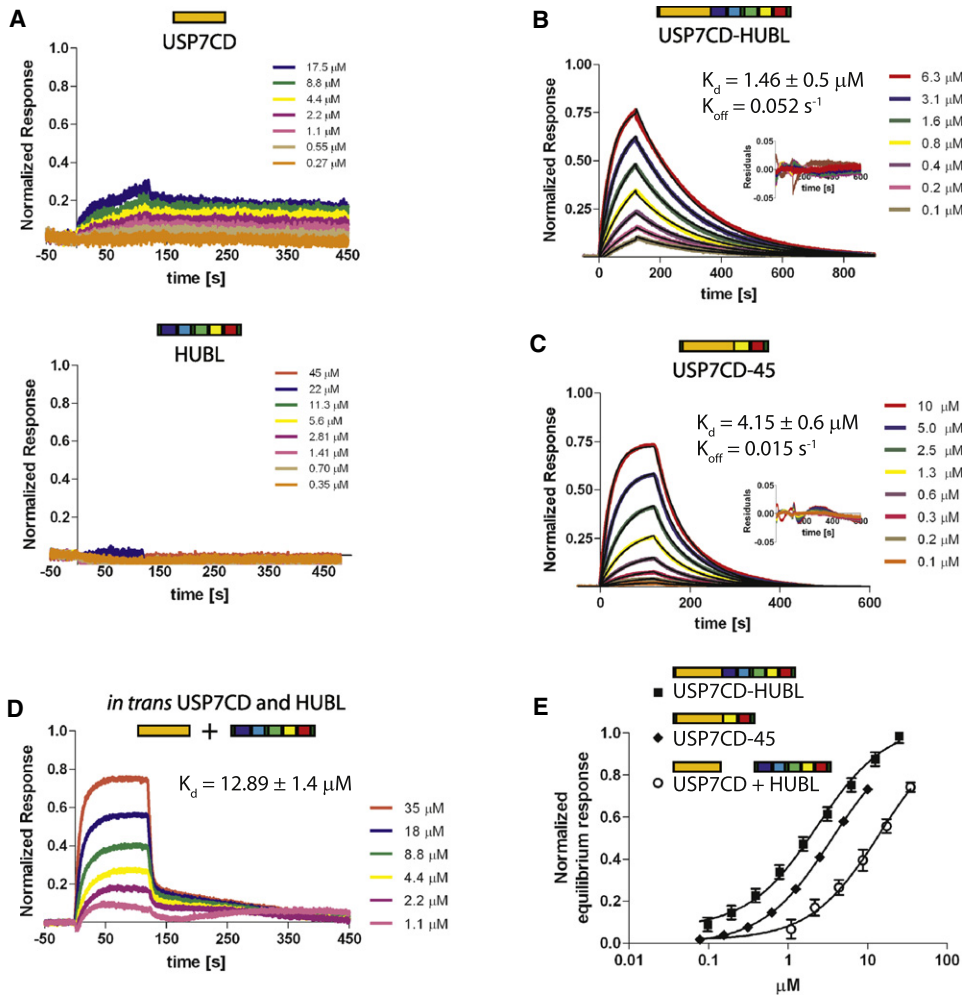

Figure 5. Ubiquitin Affinity Is Increased by the HUBL Domain

(A) SPR binding studies using GST-tagged ubiquitin showed weak ubiquitin binding for USP7CD and no responses with the HUBL domain.

(B) USP7CD-HUBL binds to ubiquitin, which could be fitted using the binding kinetics (black line) to a K_d 1.5 (±0.5) μM. The inset shows the residuals.

(C) USP7CD-45 binds ubiquitin with a dissociation constant of 4.15 (±0.6) μM. The inset shows the residuals.

(D) The dissociation constant for ubiquitin of the USP7CD is increased to 12.90 (±1.4) μM in the presence of 50 μM of the HUBL domain.

(E) Overlay of the normalized equilibrium responses.

activated state. Therefore, the HUBL activation mechanism may be susceptible to regulation. A prime candidate for this regulation is GMPS, a metabolic enzyme that binds and activates USP7 in *Drosophila* (van der Knaap et al., 2005) and humans (Sarkari et al., 2009). To analyze whether the HUBL domain intrinsically and constitutively activates USP7, or whether it can be further regulated, we studied the modulation of USP7 activity by GMPS.

First, we wondered which USP7 domains are involved in GMPS binding. Using pull-down experiments with various GST-tagged USP7 constructs, we show that GMPS binds to USP7 only when HUBL-123 is present (Figure S7A). USP7CD-HUBL, USP7CD-123, and HUBL-123 have a very tight interaction with GMPS (K_d of 30–40 nM), as shown by SPR (Figure 7A and Figures S7B and S7C). Neither USP7CD nor USP7CD-45 showed any appreciable binding to GMPS (Figure 7A and Figure S7C), confirming that HUBL-123 is sufficient for the USP7-GMPS interaction.

Next, we wanted to see if GMPS binding affects USP7 activity. Indeed, the activity of USP7CD-HUBL in Ub-AMC assays is increased 5.5-fold in the presence of GMPS (Figure 7B and Table S1). Kinetic analysis reveals an increased k_{cat}, with only a slightly increased K_M, consistent with the observation that the ubiquitin affinity of the complex does not change (K_d 2.5 ± 0.17 μM) (Figure S7D). The presence of GMPS does not activate USP7CD-123 even if they interact tightly (Figure S7E). Importantly, when we introduced the W285D E286A and I1100S mutations to USP7CD-HUBL, the mutant proteins bound GMPS equally well as the wild-type (Figures S7A–S7C) but could no longer be activated by GMPS (Figure 7C). This shows that GMPS hyperactivation of USP7 requires a functional switching loop in the catalytic domain and works through the HUBL-45-dependent activation.

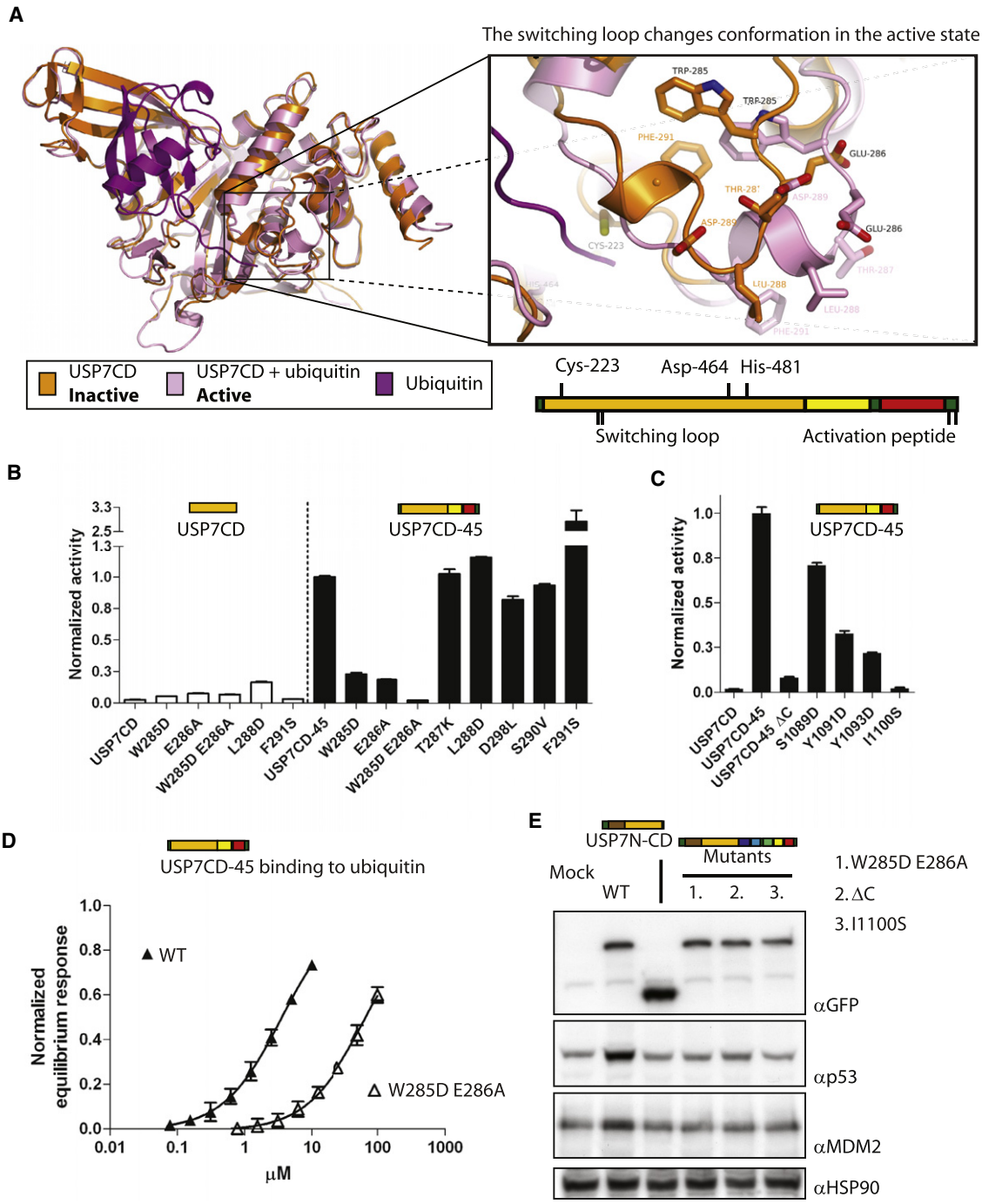

Figure 6. Mutants in the Catalytic Domain and HUBL-45 Prevent Activation

(A) Crystal structures of the USP7 catalytic domain (1NB8 and 1NBF) show a remodeling of the switching loop (residues W285–F291) and active site upon binding of ubiquitin aldehyde. Schematic diagram of USP7CD-45 shows catalytic residues, the switching loop, and activation peptide.

(B) Mutating switching loop residues W285 and E286 in the catalytic domain dramatically reduced the activity of USP7CD-45. In USP7CD a limited activating effect is seen, due to destabilization of the inactive form. Mutating F291 resulted in extra HUBL activation. The activity is normalized to full-length USP7.

(C) Mutating conserved residues in the C-terminal activation peptide of HUBL-45 resulted in decreased activity on Ub-AMC, with a complete loss of activation for mutant Ile1100Ser.

(D) SPR shows dramatic decrease in ubiquitin binding for USP7CD-45 W285D E286A (K_d = 67.9 ± 5.3 μM).

(E) USP7FL activity in U2OS cells is reduced for mutants in the switching loop (1, W285D E286A) or in the activation peptide (2, ΔC; 3, I1100S), since protein levels of p53 and MDM2 only increase with wild-type USP7. HSP90 was used as a loading control.

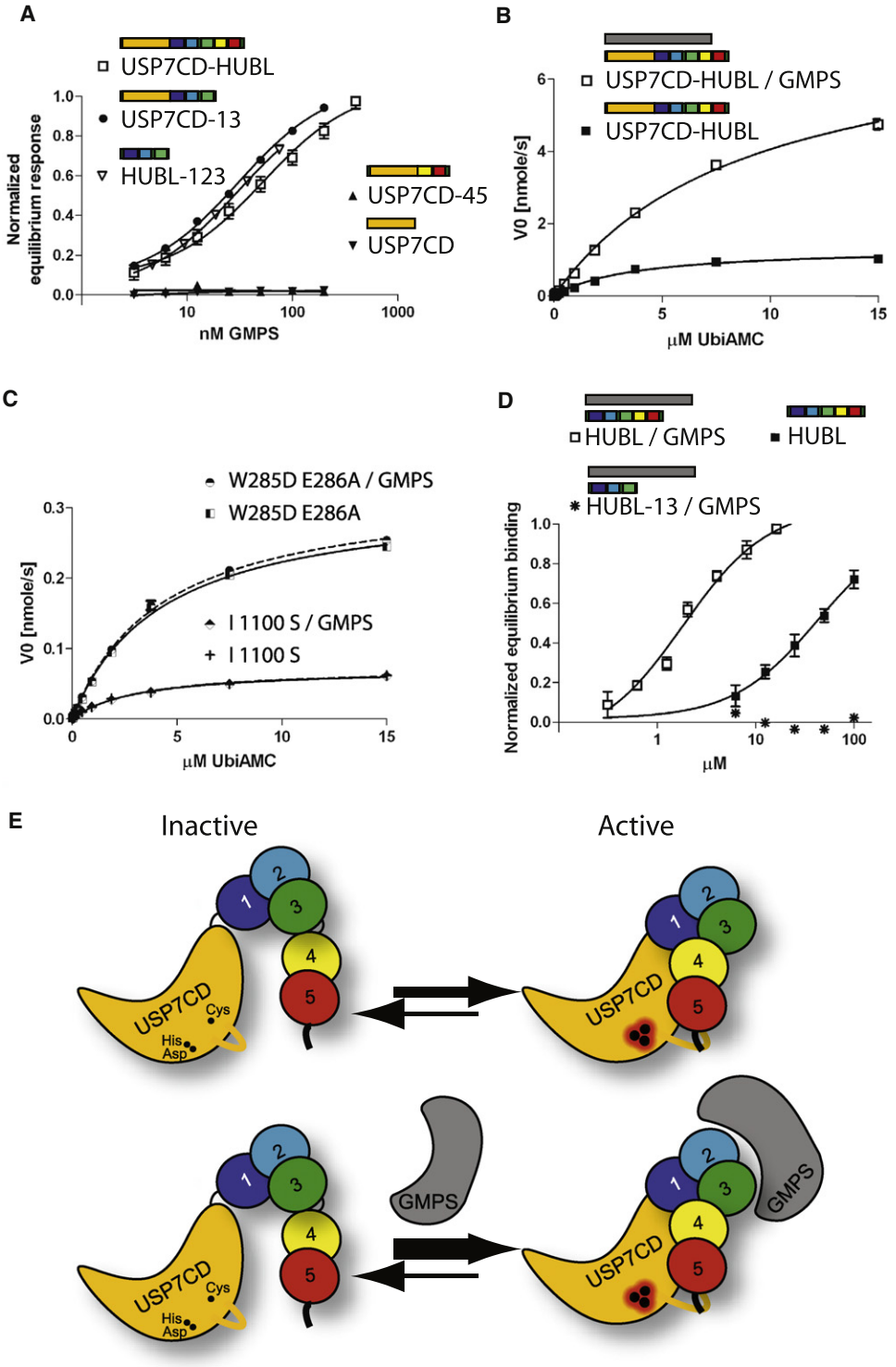

Figure 7. GMPS Can Hyperactivate the HUBL Autoactivation

(A) SPR experiments show that GMPS binds to USP7 constructs containing HUBL-123 with a K_d of 30–40 nM.

(B) Kinetic analysis of USP7CD-HUBL / GMPS complex showed a 5.5-fold increase of k_{cat}.

(C) The W285D E286A and I1100S mutants in USP7CD-HUBL (solid lines) prevent hyperactivation by GMPS (dashed lines) in the Ub-AMC assays.

(D) In complex with GMPS the binding of the HUBL domain for GST-USP7CD increased from a K_d of 48 (±9.7) μM to 1.8 (±0.42) μM.

(E) Model for the autoactivation of the USP7 catalytic domain by the HUBL domain, which is allosterically promoted by GMPS. In its resting state, the catalytic triad is in a misaligned and inactive conformation, resulting in an almost inactive enzyme. However, the HUBL-45 domain interacts with the USP7 catalytic domain

To confirm whether the GMPS-dependent activation indeed acts through HUBL-45, we analyzed whether GMPS changed the affinity of the HUBL-45 region for the catalytic domain. Strikingly, whereas the HUBL-123 has no affinity for the catalytic domain in the presence of GMPS, the dissociation constant between the full HUBL domain and the catalytic domain increases from 48 (±9.7) μM to 1.8 (±0.42) μM in the presence of GMPS (Figure 7D). This shows that GMPS can allosterically activate USP7 by binding to HUBL-123, stabilizing the contact between HUBL-45 and USP7CD, thus promoting the activated state.

DISCUSSION

We show here that the C-terminal HUBL-45 domain is required and sufficient for full activity of the USP7/HAUSP deubiquitinating enzyme. This mechanism depends on contacts between the C-terminal tail of HUBL-45 and a switching loop in the catalytic domain, which leads to organization of the active site and an increased affinity for ubiquitin. Single-point mutants in the switching loop or C-terminal tail interfere with USP7 activity in vivo and in vitro.

Apparently USP7 has the unusual ability to switch the active site between an active and an inactive state, resulting in the change in both k_{cat} and K_M. This was observed in the crystal structures of the catalytic domain, with and without ubiquitin. Most USP catalytic domains, USP8 (2GFO), USP14 (2AYN), USP4 (2Y6E), and CYLD (2VHF), do not have this nonorganized state of the catalytic triad. USP14 is activated by binding to the proteasome (Leggett et al., 2002), which is mediated by a single Ubl domain (Borodovsky et al., 2001). However, only for USP7 and Ubp8, a member of the SAGA complex, the two states are suggested based on biochemical and structural data (Kohler et al., 2010; Samara et al., 2010). Here we show USP7 is able to switch, since in *trans* activation is possible. Apparently, the prefolded catalytic domain can still be activated by the HUBL domain.

At first glance, full-length USP7 is continuously in the active state. However, we show that binding of GMPS can further activate USP7. The HUBL-123 domain, which is dispensable for USP7 intrinsic activity, serves as a binding platform for GMPS. This binding results in hyperactivation of USP7 through a mechanism that is completely dependent on a functional HUBL activation, since point mutants in this interface cannot be activated by GMPS. Rather, GMPS binding results in an increased affinity between the catalytic domain and the HUBL-45 unit of the HUBL domain, stabilizing the interaction.

Therefore we propose a model in which USP7 exists in equilibrium between an active and an inactive state (Figure 7E, top panel). The switch between states involves an increase of ubiquitin binding and remodeling of the active site and switching loop, due to interactions with the HUBL-45 domain. Allosteric interaction with GMPS stabilizes the active state, promoting the interaction between HUBL-45 and switching loop (Figure 7E, bottom panel). It does not affect ubiquitin binding or K_M but activates through k_{cat}, resulting in substantially more molecules in the active state.

Since the interaction between USP7CD and the HUBL domain is weak, and single-point mutants can completely prevent HUBL activation, USP7 is not always in the "on" state but rather displays flexibility, as seen in the SAXS experiments. That would explain how GMPS could hyperactivate USP7 through an increase of HUBL affinity for USP7CD, by serving as a molecular lock to reduce HUBL flexibility.

GMPS most likely has additional target-specific regulatory functions in cells (Sarkari et al., 2009; van der Knaap et al., 2005). Since not all USP7 is found in complex with GMPS or vice versa (van der Knaap et al., 2010), it is clear that USP7 is not always in this activated state in cells.

This opens the interesting possibility that other regulators could further modulate the interaction between the catalytic domain and the HUBL domain, either promoting the "on state," like GMPS, or by sequestering HUBL-45 from the catalytic domain and promoting the "off-state." Since USP7 is an important player in key cellular processes, such ability to 100-fold modulate—increase or decrease—catalytic efficiency provides a very fast response to external stimuli. The subsequent regulation could be achieved by posttranslational modification, by interaction with other partners (Sowa et al., 2009), or even by substrate interactions, since, e.g., MDM2 and p53 were shown to interact with the HUBL domain.

Regulation of USP catalytic activity through allosteric interaction has been observed before, e.g., for the SAGA complex, where binding of Sgf11 is necessary to maintain the catalytic residues of Ubp8 in the proteolytically active conformation (Kohler et al., 2010; Samara et al., 2010). Interestingly, this allosteric activation depends on the topologically equivalent switching loop as in USP7. Moreover, USP7 and Upb8 share the conserved W285 that is involved in the switching of USP7, confirming its importance. However, the mechanism in Ubp8 is distinct, since it relies on intermolecular interactions, rather than an intramolecular interaction as in USP7.

Surprisingly, both the activation of USP7 and the GMPS binding are conveyed by Ubl domains. None of these Ubl domains seem to resemble ubiquitin enough to compete for ubiquitin binding in the substrate binding site. This is in contrast to the internal Ubl domain in USP4, which competitively inhibits catalytic activity (Luna-Vargas et al., 2011). In USP7 the Ubl domains behave as larger units, with different functions. Although Ubl domains were predicted in other USPs, the large number of Ubl domain in the HUBL domain itself seems to be unique for USP7.

The importance of USP7 for localization and stability of critical cancer targets such as FOXO4, PTEN, and p53/MDM2 makes it into an interesting drug target. The unique features of its regulation may well offer specific opportunities for drug development.

and through its flexible C-terminal activating peptide mediates a conformational change of the switching loop, resulting in a rearrangement of the catalytic triad to the active conformation. This increases both catalytic turnover and ubiquitin affinity (top panel). Subsequent binding of GMPS allosterically stabilizes the activated state by binding to HUBL-123, in a mechanism that requires HUBL-45 and results in an increased affinity between the catalytic domain and the HUBL-45 unit of the HUBL domain (bottom panel).

EXPERIMENTAL PROCEDURES

Protein Expression and Purification

Full-length USP7 and GMPS were expressed in insect cells, USP7 truncation constructs, and mutants in *E. coli*. Proteins were purified using GST Sepharose (GE Healthcare) followed by size exclusion chromatography in 10 mM HEPES (pH 7.5), 100 mM NaCl, and 1 mM DTT. All proteins eluted from the gel filtration as monomers.

In Vitro p53 Deubiquitination Assay

Purified hyperstable p53 (Khoo et al., 2009) was ubiquitinated for 1 hr at 37°C. The reaction was stopped by adding 11 mM EDTA and incubated with varying concentrations of USP7 for 1 hr at 37°C. Western blot was performed using mouse p53 antibody (PAB240 Santa Cruz).

Cell Cultures, Transient Transfections

U2OS cells were transfected with 10 μg of the GFP-USP7 construct and 0.5 μg pBabePuro per 10 cm dish. Forty-eight hours after transfection, cells were selected with puromycin. Western blots were performed using whole-cell extracts transferred to PVDF membranes (Millipore).

Kinetic Analysis with Ubiquitin-AMC Assay

Kinetic parameters were determined using constant enzyme concentrations (1 nM for fully active USP7, else 10 nM) to hydrolyze varying substrate concentrations (from 15 μM in 2-fold dilutions). Curves were obtained by plotting enzyme initial rates (v) versus substrate concentrations ([S]) and were subjected to nonlinear regression fit using the Michaelis-Menten equation. Experimental data were processed using Prism 4.03 (GraphPad Software, Inc.).

Crystal Structure Determination

For data collection statistics and crystallographic parameters, see Table 1. HUBL was crystallized at 4°C in sitting drops against 10% (w/v) PEG4000, 200 mM sodium chloride, and 100 mM MES at pH 6.0 and supplemented with 20% (w/v) glycerol as cryoprotectant. Diffraction images were integrated with iMOSFLM (Leslie, 2006) and scaled with SCALA (Evans, 2006). Structure was solved from a selenomethionine derivative, using SHARP/autoSHARP (Vonrhein et al., 2007). ARP/wARP (Langer et al., 2008) traced 375 out of 547 residues. This model was manually completed in Coot (Emsley and Cowtan, 2004) and refined in iterative cycles with PHENIX (Adams et al., 2010) and Buster (Blanc et al., 2004).

SAXS Sample Preparation, Data Collection, and Analysis

Samples for the SAXS experiments were prepared fresh, and five samples were taken during concentration (from 0.5 to 10 mg/ml), collecting the flowthrough for blank measurements. Data were analyzed using the ATSAS software package (Svergun et al., 2001). For the HUBL domain, aggregation was observed and only the lowest concentration was used.

Surface Plasmon Resonance

SPR was performed at 25°C on a Biacore T100. A CM5 sensor chip was prepared with monoclonal GST antibody via amino coupling. Biotinylated peptides were coupled to a SA chip. Saturation binding values were plotted against concentration USP7 (GST as reference) and fit to a steady-state affinity model for calculation of apparent dissociation (Kd) constants (Prism 4.03, GraphPad Software, Inc.). All experiments have been repeated at least three times.

Extended experimental procedures are presented in the Supplemental Information.

ACCESSION NUMBERS

Coordinates and structure factors were deposited in the Protein Data Bank under identification code 2YLM.

SUPPLEMENTAL INFORMATION

Supplemental Information includes six figures, one table, Supplemental Experimental Procedures, and Supplemental References and can be found with this article online at doi:10.1016/j.molcel.2011.06.034.

ACKNOWLEDGMENTS

We thank Mirjam Epping (Bernards/Pandolfi lab) for GFP-USP7 constructs, Caroline Blair and Alan Fersht for p53, Judith Smit for ubiquitinated p53, Mark Luna-Vargas for di-ubiquitin, Remco Merkx for ubiquitin-VME and Ubiquitin-AMC, Pim van Dijk and Alex Fish for technical assistance, and Adam Round for assistance with SAXS data collection. We thank Dmitry Svergun for discussion of SAXS data; and Peter Verrijzer, Rene Bernards, and B7 and B8 group members for discussion and critical reading of the manuscript. X-ray data were collected at ESRF beamline ID23-2 (Native crystal), ID14-3 (SAXS), and SLS PX beamline (SAD). This work has been supported by grants from the Dutch Cancer Society, KWF, NWO-CW, EU-Rubicon, and EU-3D repertoire. A.C.F. designed, performed, and analyzed all in vitro experiments and wrote the manuscript. A.M.G.D. designed, performed, and analyzed all in vivo experiments. A.S. observed the increase of ubiquitin affinity for the first time using ubiquitin-isopeptide isosteres. H.O. supervised ubiquitin-isopeptide research. A.P. supervised X-ray data collection and analysis. T.K.S. designed research and supervised all in vitro experiments and manuscript writing.

Received: March 28, 2011
Revised: June 6, 2011
Accepted: June 29, 2011
Published: October 6, 2011

REFERENCES

Adams, P.D., Afonine, P.V., Bunkoczi, G., Chen, V.B., Davis, I.W., Echols, N., Headd, J.J., Hung, L.W., Kapral, G.J., Grosse-Kunstleve, R.W., et al. (2010). PHENIX: a comprehensive Python-based system for macromolecular structure solution. Acta Crystallogr. *66*, 213–221.

Becker, K., Marchenko, N.D., Palacios, G., and Moll, U.M. (2008). A role of HAUSP in tumor suppression in a human colon carcinoma xenograft model. Cell Cycle *7*, 1205–1213.

Blanc, E., Roversi, P., Vonrhein, C., Flensburg, C., Lea, S.M., and Bricogne, G. (2004). Refinement of severely incomplete structures with maximum likelihood in BUSTER-TNT. Acta Crystallogr. *60*, 2210–2221.

Boritzki, T.J., Jackson, R.C., Morris, H.P., and Weber, G. (1981). Guanosine-5′-phosphate synthetase and guanosine-5′-phosphate kinase in rat hepatomas and kidney tumors. Biochim. Biophys. Acta *658*, 102–110.

Borodovsky, A., Kessler, B.M., Casagrande, R., Overkleeft, H.S., Wilkinson, K.D., and Ploegh, H.L. (2001). A novel active site-directed probe specific for deubiquitylating enzymes reveals proteasome association of USP14. EMBO J. *20*, 5187–5196.

Burroughs, A.M., Balaji, S., Iyer, L.M., and Aravind, L. (2007). Small but versatile: the extraordinary functional and structural diversity of the beta-grasp fold. Biol. Direct *2*, 18.

Canning, M., Boutell, C., Parkinson, J., and Everett, R.D. (2004). A RING finger ubiquitin ligase is protected from autocatalyzed ubiquitination and degradation by binding to ubiquitin-specific protease USP7. J. Biol. Chem. *279*, 38160–38168.

Cummins, J.M., and Vogelstein, B. (2004). HAUSP is required for p53 destabilization. Cell Cycle *3*, 689–692.

Cummins, J.M., Rago, C., Kohli, M., Kinzler, K.W., Lengauer, C., and Vogelstein, B. (2004). Tumour suppression: disruption of HAUSP gene stabilizes p53. Nature *428*, 486.

Emsley, P., and Cowtan, K. (2004). Coot: model-building tools for molecular graphics. Acta Crystallogr. *60*, 2126–2132.

Epping, M.T., Meijer, L.A., Krijgsman, O., Bos, J.L., Pandolfi, P.P., and Bernards, R. (2011). TSPYL5 suppresses p53 levels and function by physical interaction with USP7. Nat. Cell Biol. *13*, 102–108.

Evans, P. (2006). Scaling and assessment of data quality. Acta Crystallogr. *62*, 72–82.

Fernandez-Montalvan, A., Bouwmeester, T., Joberty, G., Mader, R., Mahnke, M., Pierrat, B., Schlaeppi, J.M., Worpenberg, S., and Gerhartz, B. (2007). Biochemical characterization of USP7 reveals post-translational modification sites and structural requirements for substrate processing and subcellular localization. FEBS J. *274*, 4256–4270.

Grabbe, C., and Dikic, I. (2009). Functional roles of ubiquitin-like domain (ULD) and ubiquitin-binding domain (UBD) containing proteins. Chem. Rev. *109*, 1481–1494.

Holm, L., Kaariainen, S., Rosenstrom, P., and Schenkel, A. (2008). Searching protein structure databases with DaliLite v.3. Bioinformatics *24*, 2780–2781.

Hong, S., Kim, S.J., Ka, S., Choi, I., and Kang, S. (2002). USP7, a ubiquitin-specific protease, interacts with ataxin-1, the SCA1 gene product. Mol. Cell. Neurosci. *20*, 298–306.

Hu, M., Li, P., Li, M., Li, W., Yao, T., Wu, J.W., Gu, W., Cohen, R.E., and Shi, Y. (2002). Crystal structure of a UBP-family deubiquitinating enzyme in isolation and in complex with ubiquitin aldehyde. Cell *111*, 1041–1054.

Hu, M., Gu, L., Li, M., Jeffrey, P.D., Gu, W., and Shi, Y. (2006). Structural basis of competitive recognition of p53 and MDM2 by HAUSP/USP7: implications for the regulation of the p53-MDM2 pathway. PLoS Biol. *4*, e27. 10.1371/journal.pbio.0040027.

Khoo, K.H., Joerger, A.C., Freund, S.M., and Fersht, A.R. (2009). Stabilising the DNA-binding domain of p53 by rational design of its hydrophobic core. Protein Eng. Des. Sel. *22*, 421–430.

Kohler, A., Zimmerman, E., Schneider, M., Hurt, E., and Zheng, N. (2010). Structural basis for assembly and activation of the heterotetrameric SAGA histone H2B deubiquitinase module. Cell *141*, 606–617.

Komander, D., Lord, C.J., Scheel, H., Swift, S., Hofmann, K., Ashworth, A., and Barford, D. (2008). The structure of the CYLD USP domain explains its specificity for Lys63-linked polyubiquitin and reveals a B box module. Mol. Cell *29*, 451–464.

Kon, N., Kobayashi, Y., Li, M., Brooks, C.L., Ludwig, T., and Gu, W. (2010). Inactivation of HAUSP in vivo modulates p53 function. Oncogene *29*, 1270–1279.

Krissinel, E., and Henrick, K. (2004). Secondary-structure matching (SSM), a new tool for fast protein structure alignment in three dimensions. Acta Crystallogr. *60*, 2256–2268.

Langer, G., Cohen, S.X., Lamzin, V.S., and Perrakis, A. (2008). Automated macromolecular model building for X-ray crystallography using ARP/wARP version 7. Nat. Protoc. *3*, 1171–1179.

Leggett, D.S., Hanna, J., Borodovsky, A., Crosas, B., Schmidt, M., Baker, R.T., Walz, T., Ploegh, H., and Finley, D. (2002). Multiple associated proteins regulate proteasome structure and function. Mol. Cell *10*, 495–507.

Leslie, A.G. (2006). The integration of macromolecular diffraction data. Acta Crystallogr. *62*, 48–57.

Li, M., Chen, D., Shiloh, A., Luo, J., Nikolaev, A.Y., Qin, J., and Gu, W. (2002). Deubiquitination of p53 by HAUSP is an important pathway for p53 stabilization. Nature *416*, 648–653.

Li, M., Brooks, C.L., Kon, N., and Gu, W. (2004). A dynamic role of HAUSP in the p53-Mdm2 pathway. Mol. Cell *13*, 879–886.

Luna-Vargas, M.P., Faesen, A.C., van Dijk, W.J., Rape, M., Fish, A., and Sixma, T.K. (2011). Ubiquitin-specific protease 4 is inhibited by its ubiquitin-like domain. EMBO Rep. *12*, 365–372.

Ma, J., Martin, J.D., Xue, Y., Lor, L.A., Kennedy-Wilson, K.M., Sinnamon, R.H., Ho, T.F., Zhang, G., Schwartz, B., Tummino, P.J., and Lai, Z. (2010). C-terminal region of USP7/HAUSP is critical for deubiquitination activity and contains a second mdm2/p53 binding site. Arch. Biochem. Biophys. *503*, 207–212.

Madsen, L., Schulze, A., Seeger, M., and Hartmann-Petersen, R. (2007). Ubiquitin domain proteins in disease. BMC Biochem. *8* (*Suppl 1*), S1.

Marchenko, N.D., Wolff, S., Erster, S., Becker, K., and Moll, U.M. (2007). Monoubiquitylation promotes mitochondrial p53 translocation. EMBO J. *26*, 923–934.

Meulmeester, E., Maurice, M.M., Boutell, C., Teunisse, A.F., Ovaa, H., Abraham, T.E., Dirks, R.W., and Jochemsen, A.G. (2005). Loss of HAUSP-mediated deubiquitination contributes to DNA damage-induced destabilization of Hdmx and Hdm2. Mol. Cell *18*, 565–576.

Nijman, S.M., Luna-Vargas, M.P., Velds, A., Brummelkamp, T.R., Dirac, A.M., Sixma, T.K., and Bernards, R. (2005). A genomic and functional inventory of deubiquitinating enzymes. Cell *123*, 773–786.

Samara, N.L., Datta, A.B., Berndsen, C.E., Zhang, X., Yao, T., Cohen, R.E., and Wolberger, C. (2010). Structural insights into the assembly and function of the SAGA deubiquitinating module. Science *328*, 1025–1029.

Saridakis, V., Sheng, Y., Sarkari, F., Holowaty, M.N., Shire, K., Nguyen, T., Zhang, R.G., Liao, J., Lee, W., Edwards, A.M., et al. (2005). Structure of the p53 binding domain of HAUSP/USP7 bound to Epstein-Barr nuclear antigen 1 implications for EBV-mediated immortalization. Mol. Cell *18*, 25–36.

Sarkari, F., Sanchez-Alcaraz, T., Wang, S., Holowaty, M.N., Sheng, Y., and Frappier, L. (2009). EBNA1-mediated recruitment of a histone H2B deubiquitylating complex to the Epstein-Barr virus latent origin of DNA replication. PLoS Pathog. *5*, e1000624. 10.1371/journal.ppat.1000624.

Sarkari, F., Sheng, Y., and Frappier, L. (2010). USP7/HAUSP promotes the sequence-specific DNA binding activity of p53. PLoS ONE *5*, e13040. 10.1371/journal.pone.0013040.

Sheng, Y., Saridakis, V., Sarkari, F., Duan, S., Wu, T., Arrowsmith, C.H., and Frappier, L. (2006). Molecular recognition of p53 and MDM2 by USP7/HAUSP. Nat. Struct. Mol. Biol. *13*, 285–291.

Song, M.S., Carracedo, A., Salmena, L., Song, S.J., Egia, A., Malumbres, M., and Pandolfi, P.P. (2011). Nuclear PTEN regulates the APC-CDH1 tumor-suppressive complex in a phosphatase-independent manner. Cell *144*, 187–199.

Sowa, M.E., Bennett, E.J., Gygi, S.P., and Harper, J.W. (2009). Defining the human deubiquitinating enzyme interaction landscape. Cell *138*, 389–403.

Svergun, D.I., Petoukhov, M.V., and Koch, M.H. (2001). Determination of domain structure of proteins from X-ray solution scattering. Biophys. J. *80*, 2946–2953.

Trotman, L.C., Wang, X., Alimonti, A., Chen, Z., Teruya-Feldstein, J., Yang, H., Pavletich, N.P., Carver, B.S., Cordon-Cardo, C., Erdjument-Bromage, H., et al. (2007). Ubiquitination regulates PTEN nuclear import and tumor suppression. Cell *128*, 141–156.

van der Horst, A., de Vries-Smits, A.M., Brenkman, A.B., van Triest, M.H., van den Broek, N., Colland, F., Maurice, M.M., and Burgering, B.M. (2006). FOXO4 transcriptional activity is regulated by monoubiquitination and USP7/HAUSP. Nat. Cell Biol. *8*, 1064–1073.

van der Knaap, J.A., Kumar, B.R., Moshkin, Y.M., Langenberg, K., Krijgsveld, J., Heck, A.J., Karch, F., and Verrijzer, C.P. (2005). GMP synthetase stimulates histone H2B deubiquitylation by the epigenetic silencer USP7. Mol. Cell *17*, 695–707.

van der Knaap, J.A., Kozhevnikova, E., Langenberg, K., Moshkin, Y.M., and Verrijzer, C.P. (2010). Biosynthetic enzyme GMP synthetase cooperates with ubiquitin-specific protease 7 in transcriptional regulation of ecdysteroid target genes. Mol. Cell. Biol. *30*, 736–744.

Vogelstein, B., Lane, D., and Levine, A.J. (2000). Surfing the p53 network. Nature *408*, 307–310.

Vonrhein, C., Blanc, E., Roversi, P., and Bricogne, G. (2007). Automated structure solution with autoSHARP. Methods Mol. Biol. *364*, 215–230.

Weber, G., Burt, M.E., Jackson, R.C., Prajda, N., Lui, M.S., and Takeda, E. (1983). Purine and pyrimidine enzymic programs and nucleotide pattern in sarcoma. Cancer Res. *43*, 1019–1023.

Zhu, X., Menard, R., and Sulea, T. (2007). High incidence of ubiquitin-like domains in human ubiquitin-specific proteases. Proteins *69*, 1–7.